ARTICLE IN PRESS

PERGAMON

Chaos, Solitons and Fractals 15 (2003) 219–232

CHAOS
SOLITONS & FRACTALS

www.elsevier.com/locate/chaos

Low-dimensional chaos in high-dimensional phase space: how does it occur?

Ying-Cheng Lai [a,b,*], Erik M. Bollt [c], Zonghua Liu [a]

[a] *Department of Mathematics, Center for Systems Science and Engineering Research, Arizona State University, Tempe, AZ 85287-1804, USA*

[b] *Department of Electrical Engineering and Physics, Arizona State University, Tempe, AZ 85287-1804, USA*

[c] *Department of Mathematics, 572 Holloway Road, United States Naval Academy, Annapolis, MD 21402, USA*

Accepted 29 April 2002

Abstract

A fundamental observation in nonlinear dynamics is that the asymptotic chaotic invariant sets in many high-dimensional systems are low-dimensional. We argue that such a behavior is typically associated with chaos synchronism. Numerical support using coupled chaotic systems including a class derived from a nonlinear partial differential equation is provided.

1. Introduction

The phase spaces of many dynamical systems in nature, such as those described by nonlinear partial differential equations (PDEs), are infinite-dimensional. Yet it often occurs that the dynamical invariant sets responsible for many observable phenomena of physical interest lie in some low-dimensional manifold, as speculated by Ruelle and Takens in 1971 [1] and later verified in many natural systems [2]. The hope that low-dimensional chaos may be relevant to high-dimensional dynamical systems is one reason that drives not only theoretical chaos research such as differentiable dynamics [3], but also applied work such as chaotic time series analysis [4]. In this paper we shall argue that chaos synchronism [5,6] provides a natural and fundamental mechanism for high-dimensional systems to exhibit low-dimensional chaos.

Throughout the paper we adopt the notion that low-dimensional chaos is characterized by only one positive Lyapunov exponent while high-dimensional chaos by more than one such exponent. Consider a class of dynamical systems described by

$$d\mathbf{X}/dt = \mathbf{F}(\mathbf{X}, \mathbf{p}), \tag{1}$$

where $\mathbf{X} \in \mathbf{R}^N$, $N \gg 1$ is the phase-space dimension, and $\mathbf{p}$ denotes a set of system parameters. Despite high dimensionality of the phase space, often, there exist regions in the parameter space with positive Lebesgue measure in which the asymptotic dynamical invariant set is d-dimensional, where $d \ll N$. That is, there exists an invariant manifold of dimension m, where $m \gtrsim d$, in which the invariant set is embedded. Let $\mathcal{M}$ denote this low-dimensional manifold. Our point is that, when a high-dimensional dynamical system exhibits low-dimensional chaotic behaviors, the dynamical

* Corresponding author. Address: Department of Mathematics, Center for Systems Science and Engineering Research, Arizona State University, Tempe, AZ 85287-1804, USA. Fax: +1-480-965-0461.

E-mail address: yclai@chaos1.la.asu.edu (Y.-C. Lai).

0960-0779/03/$ - see front matter
PII: S0960-0779(02)00094-2

variables $\mathbf{X}$ in the original high-dimensional phase space will generally be synchronized with the variables in $\mathscr{M}$. Let $\mathbf{x} \in \mathscr{M} \subseteq \mathbf{R}^m$ be the set of dynamical variables in $\mathscr{M}$. Then, as we shall argue in this paper, synchronization between $\mathbf{X}$ and $\mathbf{x}$ is a sufficient condition for the asymptotic dynamics of the original high-dimensional system to be low-dimensional. Generally, this synchronization can be expressed by the following function that is not necessarily smooth:

$$\mathbf{X} = \mathbf{g}(\mathbf{x}), \quad \text{where } \mathbf{g} : \mathbf{R}^N \to \mathbf{R}^m. \tag{2}$$

To facilitate analysis and numerical computation, we investigate a class of coupled chaotic systems, including a class of such systems derived from a nonlinear PDE [7]. We will provide numerical evidence that as a system parameter changes, the onset of low-dimensional chaos coincides with the parameter value at which the synchronization state becomes stable. An implication of our results is that the phenomenon of chaotic synchronization [5,6], besides its importance in technological applications [8,9], is more fundamental than previously indicated in the chaotic dynamics literature.

It is important, at this point, to discuss our work versus the "slaving principle" in the context of *synergetics* proposed by Haken in the seventies [10]. Mathematically, the slaving principle is represented by Eq. (2). Briefly, synergetics deals with systems composed of many subsystems and studies how the interaction (or "cooperation", as called by Haken) among these subsystems brings about spatial, temporal or functional structures on macroscopic scales. Particular attention is focused on situations where these structures arise in a self-organized fashion, and governed by the slaving principle. The slaving principle implies reduction in dimensionality, which contains a number of important theorems as special cases, such as the center manifold theorem, the slow manifold theorem, and adiabatic elimination procedures [10]. Its main content is to use the adiabatic approximation to remove the fast variable and find the order parameter equation (slow variable). The order parameters determine the type and degree of order. Our point is that, synergetics addresses mainly the collective behavior in coupled limit-cycle systems. More importantly, the existing point of view is that the slaving principle in synergetics is not applicable to chaotic systems [11]. Our work deals with, *exclusively*, dimension reduction in chaotic systems and, therefore, is novel beyond what can be understood in the context of synergetics.

The paper is organized as follows. In Section 2, we provide a simple argument for the interplay between the onset of low-dimensional chaotic behavior and the stability of the synchronization state. In Section 3, we present numerical examples with the system of coupled Rössler oscillators [12]. In Section 4, we study a model of coupled chaotic oscillators derived from a nonlinear PDE. In Section 5, we investigate a model consisting of two coupled, but characteristically different chaotic maps to illustrate the interplay between generalized synchronism and the occurrence of low-dimensional chaos. A brief discussion is presented in Section 6.

2. Synchronism and onset of low-dimensional chaos

2.1. Generalized synchronization as a typical mechanism for low-dimensional chaos

We argue that synchronism is a sufficient condition for the occurrence of low-dimensional chaotic dynamics by considering the following unidirectionally coupled system:

$$\frac{\mathrm{d}\mathbf{x}}{\mathrm{d}t} = \mathbf{f}(\mathbf{x}), \quad \frac{\mathrm{d}\mathbf{y}}{\mathrm{d}t} = \mathbf{g}(\mathbf{x}, \mathbf{y}), \tag{3}$$

where the $\mathbf{x}$-dynamics admits a low-dimensional chaotic attractor with one positive Lyapunov exponent $\Lambda_1^x > 0$. By synchronization we mean the existence of a functional relation between the set of driving variables $\mathbf{x}$ and the set of driven variables $\mathbf{y}$

$$\mathbf{y} = \mathbf{h}(\mathbf{x}). \tag{4}$$

This function also defines the synchronization manifold $\mathscr{M}$, and the synchronization is *generalized* [13]. Eq. (3) has been shown to be a sufficient representation of coupled nonlinear oscillators in general, because there always exists a mathematical change of coordinates to transform a pair of mutually coupled (bidirectionally coupled) oscillators into a pair of unidirectionally coupled ones, at least locally near the synchronization manifold [14]. Since the $\mathbf{x}$-subsystem already has one positive Lyapunov exponent, the full system Eq. (3) is high-dimensionally chaotic if the $\mathbf{y}$-subsystem possesses at least one positive Lyapunov exponent. Otherwise, Eq. (3) is low-dimensionally chaotic if the largest Lyapunov exponent of the $\mathbf{y}$-subsystem is not positive. This exponent is given by

$$\Lambda_1^y = \lim_{t\to\infty} \frac{1}{t} \ln \frac{|\delta\mathbf{y}(t)|}{|\delta\mathbf{y}(0)|}, \tag{5}$$

where $\delta\mathbf{y}(0)$ is a randomly chosen initial infinitesimal vector in the tangent space of the **y**-subsystem, and the evolution of this vector is governed by

$$\frac{\mathrm{d}\delta\mathbf{y}(t)}{\mathrm{d}t} = \frac{\partial\mathbf{g}}{\partial\mathbf{y}} \cdot \delta\mathbf{y}(t), \tag{6}$$

where the Jacobian matrix $\partial\mathbf{g}/\partial\mathbf{y}$ is evaluated with respect to a trajectory in the full phase space. On the other hand, the stability of the synchronization manifold $\mathscr{M}$ is determined by the following *transverse* Lyapunov exponent:

$$\Lambda_{\mathrm{T}} = \lim_{t\to\infty} \frac{1}{t} \ln \frac{|\delta\mathbf{y}(t)|}{|\delta\mathbf{y}(0)|}\bigg|_{\mathbf{y}=\mathbf{h}(\mathbf{x})}, \tag{7}$$

where the Jacobian matrix $\partial\mathbf{g}/\partial\mathbf{y}$ now is evaluated locally at $\mathscr{M}$. When $\mathscr{M}$ is transversely stable so that synchronization is achieved, we have $\Lambda_{\mathrm{T}} < 0$. But then, asymptotically a trajectory lies in $\mathscr{M}$ and, hence, $\Lambda_1^y = \Lambda_{\mathrm{T}} < 0$. Thus, in this case, there is no positive Lyapunov exponent in the **y**-subsystem and the full system Eq. (3) is low-dimensionally chaotic. However, $\Lambda_1^y < 0$ does not necessarily imply that $\Lambda_{\mathrm{T}} < 0$. Therefore, *generalized synchronism is a sufficient but not a necessary condition for the occurrence of low-dimensional chaotic dynamics*. This statement is true under the assumptions of Eq. (3), which are: (1) the **y**-variables can synchronize to the **x**-variables in a generalized sense, and (2) the **x**-variables admit only one positive Lyapunov exponent.

2.2. System of coupled, identical chaotic oscillators

The above consideration can be easily extended to one common class of spatiotemporal systems: coupled chaotic oscillators. A simple system consisting of two such oscillators can be written, as follows:

$$\begin{aligned} \frac{\mathrm{d}\mathbf{x}}{\mathrm{d}t} &= \mathbf{f}_1(\mathbf{x}) + \epsilon \cdot (\mathbf{y} - \mathbf{x}), \\ \frac{\mathrm{d}\mathbf{y}}{\mathrm{d}t} &= \mathbf{f}_2(\mathbf{y}) + \epsilon \cdot (\mathbf{x} - \mathbf{y}) \end{aligned} \tag{8}$$

where $\mathbf{x} \in \mathbf{R}^m$ and $\mathbf{y} \in \mathbf{R}^m$, $\mathbf{f}_1$ and $\mathbf{f}_2$ are velocity fields of the chaotic flows $\mathbf{x}(t)$ and $\mathbf{y}(t)$, respectively, and ϵ denotes the coupling matrix.

We consider the case where the oscillators are identical: $\mathbf{f}_1 = \mathbf{f}_2 \equiv \mathbf{f}$, and the velocity field $\mathbf{f}(\mathbf{x})$ generates a low-dimensional chaotic attractor. In this case, the synchronization manifold $\mathscr{M}$, defined by $\mathbf{x}(t) = \mathbf{y}(t)$, is an invariant manifold of Eq. (8) in the sense that if the system is started with initial condition $\mathbf{x}(0) = \mathbf{y}(0)$, then $\mathbf{x}(t) = \mathbf{y}(t)$ holds for all $t > 0$. The transverse stability of $\mathscr{M}$ can be explicitly determined by introducing the following transform of variables:

$$(\mathbf{u}, \mathbf{v}) = \left[\tfrac{1}{2}(\mathbf{x} + \mathbf{y}), \tfrac{1}{2}(\mathbf{x} - \mathbf{y})\right], \tag{9}$$

so the synchronization state is represented by $\mathbf{v} = \mathbf{0}$. Near $\mathscr{M}$, we have $|\mathbf{v}| \sim 0$ and, to first order in $|\mathbf{v}|$, the differential equations for **u** and **v** are

$$\begin{aligned} \frac{\mathrm{d}\mathbf{u}}{\mathrm{d}t} &\approx \mathbf{f}(\mathbf{u}), \\ \frac{\mathrm{d}\mathbf{v}}{\mathrm{d}t} &\approx \left[\frac{\partial\mathbf{f}}{\partial\mathbf{u}} - 2\epsilon\right] \cdot \mathbf{v}. \end{aligned} \tag{10}$$

We see that in $\mathscr{M}$ ($\mathbf{v} = \mathbf{0}$), there is a chaotic attractor generated by **f**. The Lyapunov exponents evaluated with respect to the Jacobian matrices $[\partial\mathbf{f}/\partial\mathbf{u} - 2\epsilon]$ determine the transverse stability of chaotic trajectories in $\mathscr{M}$. When $\epsilon = \mathbf{0}$ (no coupling), $\mathscr{M}$ is transversely unstable because the transverse Lyapunov spectrum is identical to that of the chaotic flow. As the coupling parameter ϵ is increased, we expect the transverse Lyapunov exponents to decrease. For randomly chosen initial conditions, synchronization can occur when ϵ is increased through a critical value ϵ_{c} so that the largest Lyapunov exponent in **v** becomes negative. When this occurs, the asymptotic attractor of the system lies in $\mathscr{M}$ and is therefore low-dimensional. For the full system Eq. (8), for small coupling, there are two positive Lyapunov exponents. We expect then that, as ϵ is increased through ϵ_{c}, the second largest positive exponent becomes negative and, hence, precisely at ϵ_{c}, there is a transition from high-dimensional to low-dimensional chaos.

The situation of N coupled, *identical*, chaotic oscillators can be formulated in a similar way [15]. Such a system can be described as follows:

$$\frac{\mathrm{d}\mathbf{x}^i}{\mathrm{d}t} = \mathbf{f}(\mathbf{x}^i) + \epsilon \sum_{j=1}^{N} G_{ij}\mathbf{H}(\mathbf{x}^j), \quad i = 1, \ldots, N, \tag{11}$$

where G_{ij}'s are elements of the coupling matrix $\mathbf{G}$ and $\mathbf{H}(\mathbf{x})$ is a smooth function. The synchronization manifold $\mathscr{M}$ of the network is defined by: $\mathbf{x}^1 = \mathbf{x}^2 = \cdots = \mathbf{x}^N$. If G_{ij}'s satisfy the condition $\sum_j G_{ij} = 0$ for all i, a situation treated commonly in literature [15], then $\mathscr{M}$ is an invariant subspace of Eq. (11) (not necessarily stable for all ϵ). The stability of $\mathscr{M}$ can be assessed by examining the variation equation for Eq. (11), as follows:

$$\frac{\mathrm{d}\delta\mathbf{x}^i}{\mathrm{d}t} = \mathrm{D}\mathbf{f}(\mathbf{x}_n^i)\cdot\delta\mathbf{x}^i + \epsilon \sum_{j=1}^{N} G_{ij}\mathrm{D}\mathbf{H}(\mathbf{x}^i)\cdot\delta\mathbf{x}^j, \tag{12}$$

where $\mathrm{D}\mathbf{F}$ and $\mathrm{D}\mathbf{H}$ denote the partial derivatives. On $\mathscr{M}$, where $\mathbf{x}^1 = \cdots = \mathbf{x}^N = \mathbf{x}$, this can be written concisely as

$$\frac{\mathrm{d}\delta\mathbf{X}}{\mathrm{d}t} = [\mathbf{I}_N \otimes \mathrm{D}\mathbf{F}(\mathbf{x}) + \epsilon\mathbf{G}\otimes\mathrm{D}\mathbf{H}(\mathbf{x})]\cdot\delta\mathbf{X}, \tag{13}$$

where $\delta\mathbf{X} = (\delta\mathbf{x}^1, \ldots, \delta\mathbf{x}^N)^{\mathrm{T}}$, and $\mathbf{I}_N$ denotes the $N\times N$ identity matrix. If $\mathbf{G} = \mathbf{T}^{-1}\mathbf{\Gamma}T$ with $\mathbf{\Gamma} = \mathrm{Diag}(\gamma_0, \ldots, \gamma_{N-1})$, then system (13) can be decoupled into the following block diagonal form:

$$\frac{\mathrm{d}\delta Y}{\mathrm{d}t} = [\mathbf{I}_N \otimes \mathrm{D}\mathbf{F}(\mathbf{x}) + \epsilon\mathbf{\Gamma}\otimes\mathrm{D}\mathbf{H}(\mathbf{x})]\cdot\delta\mathbf{Y}, \tag{14}$$

where $\delta\mathbf{Y} = (\delta\mathbf{y}^1, \ldots, \delta\mathbf{y}^N)^{\mathrm{T}}$ and $\delta\mathbf{y}^i = \sum_j T_j^i\delta\mathbf{x}^j$. In terms of the individual components, we have N variational equations in $\mathbf{R}^m$

$$\frac{\delta\mathbf{y}^k}{\mathrm{d}t} = [\mathrm{D}\mathbf{F}(\mathbf{x}) + \epsilon\gamma_k\mathrm{D}\mathbf{H}(\mathbf{x})]\cdot\delta\mathbf{y}^k, \quad k = 0, 1, \ldots, N-1. \tag{15}$$

Note that the condition $\sum_j G_{ij} = 0$ implies that G has at least one zero eigenvalue, which we take to be γ_0; the corresponding equation determines the Lyapunov exponents of the chaotic attractor in $\mathscr{M}$. The remaining $N-1$ equations determine the stability of the orbit in the $m(N-1)$ directions transverse to $\mathscr{M}$. Our point is, as the coupling parameter ϵ is increased from zero, the number of positive Lyapunov exponent of the full system Eq. (11) becomes one at precisely the same critical parameter value ϵ_c at which the largest transverse Lyapunov exponent becomes negative.

2.3. Coupled nonidentical chaotic oscillators

When the coupled chaotic oscillators are not identical, the synchronization manifold $\mathscr{M}$ defined by $\mathbf{x}^1 = \mathbf{x}^2 = \cdots = \mathbf{x}^N$ will typically not be an invariant subspace of the system and, hence, the calculation of transverse Lyapunov exponents, as defined above, is no longer valid. In this case, the synchronization state can be more complicated, such as time-lagged synchronization observed in the system of two coupled nonidentical Rössler oscillators [16].

To gain insight, we again consider Eq. (8), but this time without invoking the assumption that the oscillators are identical. If the chaotic velocity fields are close: $\mathbf{f}_1 \approx \mathbf{f}_2$, then the synchronization state is: $\mathbf{v} = \frac{1}{2}(\mathbf{x}-\mathbf{y}) \approx \mathbf{0}$. The pair of differential equations in the $(\mathbf{u},\mathbf{v})$-variables are:

$$\begin{aligned}\frac{\mathrm{d}\mathbf{u}}{\mathrm{d}t} &\approx [\mathbf{f}_1(\mathbf{u}) + \mathbf{f}_2(\mathbf{u})]/2,\\ \frac{\mathrm{d}\mathbf{v}}{\mathrm{d}t} &\approx [\mathbf{G}(\mathbf{u}) - 2\epsilon]\cdot\mathbf{v} + [\mathbf{f}_1(\mathbf{u}) - \mathbf{f}_2(\mathbf{u})]/2,\end{aligned} \tag{16}$$

where $\mathbf{G}(\mathbf{u})$ is the average Jacobian matrix of the velocity fields $\mathbf{f}_1$ and $\mathbf{f}_2$. We see that the evolution of $\mathbf{u}(t)$ is determined by the "average" velocity field of $\mathbf{f}_1$ and $\mathbf{f}_2$. Due to the presence of the term $[\mathbf{f}_1(\mathbf{u}) - \mathbf{f}_2(\mathbf{u})]/2$ in the second equation, $\mathbf{v} = \mathbf{0}$ is no longer a solution of the system. In general, if the coupling is large enough so that the product of matrices $[\mathbf{G}(\mathbf{u}) - 2\epsilon]$ is stable, we expect $\mathbf{v}$ to stay near $\mathbf{0}$. Synchronization between the $\mathbf{x}$ and $\mathbf{y}$ systems is thus characterized by

$$\mathbf{x}(t) = \mathbf{y}(t) + 2\mathbf{v}(t), \tag{17}$$

where $|\mathbf{v}(t)| \approx 0$. Thus, as ϵ is increased, we expect that the onset of low-dimensional chaos to occur at the same value of the coupling parameter at which the average value of $\langle\mathbf{x}(t) - \mathbf{y}(t)\rangle$ becomes small. As we will show in numerical experiments, such a synchronism may manifest itself in the form of chaotic time-lagged synchronization.

3. Example: system of coupled Rössler oscillators

We consider the following system of N coupled Rössler oscillators with periodic boundary conditions:

$$\begin{aligned} \mathrm{d}x_i/\mathrm{d}t &= -\omega_i y_i - z_i + \epsilon(x_{i+1} + x_{i-1} - 2x_i), \\ \mathrm{d}y_i/\mathrm{d}t &= \omega_i x_i + a y_i, \\ \mathrm{d}z_i/\mathrm{d}t &= b + z_i(x_i - c), \end{aligned} \tag{18}$$

where ω_i ($i = 1, \ldots, N$) is the mean frequency of the ith oscillator, ϵ is the coupling parameter, and a, b, and c are the parameters of the individual Rössler oscillator. We choose $a = 0.165$, $b = 0.2$, $c = 10.0$, and $\omega_i \approx 1.0$ so that each oscillator, when uncoupled, exhibits a chaotic attractor with one positive Lyapunov exponent [12]. In what follows we treat two cases: identical and nonidentical coupled oscillators.

3.1. Identical Rössler oscillators

We set $\omega_i \equiv \omega = 1.0$ and $N = 3$. The matrix $\mathbf{G}$ and the coupling function $\mathbf{H}(\mathbf{x})$ in Eq. (11) are:

$$\mathbf{G} = \begin{pmatrix} -2 & 1 & 1 \\ 1 & -2 & 1 \\ 1 & 1 & -2 \end{pmatrix}, \quad \text{and} \quad \mathbf{H}(\mathbf{x}) = \begin{pmatrix} x \\ 0 \\ 0 \end{pmatrix}. \tag{19}$$

Since the oscillators, are identical, the simple coupling scheme defined by the matrix $\mathbf{G}$ stipulates that the three-dimensional synchronization manifold

$$\mathscr{M} : (x_1, y_1, z_1) = (x_2, y_2, z_2) = (x_3, y_3, z_3) \equiv (x, y, z)$$

be an invariant subspace of Eq. (18). The transverse subspace $\mathscr{T}$ is then six-dimensional, and so the number of transverse Lyapunov exponents is six. The Jacobian matrix that determines the transverse Lyapunov spectrum is given by

$$\mathbf{DJ}_{\mathrm{T}}(x, y, z) = \begin{pmatrix} \gamma_k \epsilon & -\omega & -1 \\ \omega & a & 0 \\ z & 0 & x - c \end{pmatrix}, \tag{20}$$

where γ_k's ($k = 0, 1, 2$) are the eigenvalues of $\mathbf{G}$: $\gamma_0 = 0$ and $\gamma_1 = \gamma_2 = -3$. The trivial eigenvalue γ_0 determines the Lyapunov spectrum of the chaotic attractor in $\mathscr{M}$, and the nontrivials ones: γ_1 and γ_2 determine the transverse spectrum. Due to degeneracy, there are only three distinct transverse Lyapunov exponents. Fig. 1(a) shows the two largest transverse exponents Λ_{T}^1 and Λ_{T}^2 (solid lines) versus the coupling parameter ϵ for $0 \leqslant \epsilon \leqslant 0.2$, where 1000 values of ϵ are

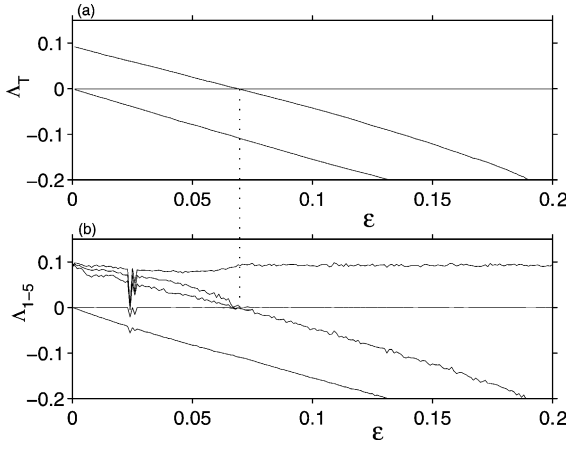

Fig. 1. For Eq. (18) with $N = 3$ (system of three coupled identical Rössler oscillators): (a) the first two distinct transverse Lyapunov exponents versus ϵ, and (b) the first five Lyapunov exponents versus ϵ. The transition to low-dimensional chaos coincides with the onset of synchronous chaos.

chosen from this interval and 10^7 time steps of $h = 0.01$ are used to compute the spectrum for each value of ϵ. We see that $\epsilon_c^T \approx 0.065$, where for $\epsilon > \epsilon_c^T$, $\mathscr{M}$ becomes transversely stable ($\Lambda_T^1 < 0$) and we expect trajectories initiating in the vicinity of $\mathscr{M}$ to approach asymptotically to $\mathscr{M}$.

When does low-dimensional chaos occur for the nine-dimensional system of Eq. (18)? Qualitatively, we note that at weak coupling ($\epsilon \gtrsim 0$), the three coupled Rössler attractors are nearly independent of each other, so the system is high-dimensionally chaotic because there are three positive Lyapunov exponents. If the coupling is strong, the three oscillators are synchronized so that there is only one Lyapunov exponent (low-dimensional chaos). The transition from high-dimensional to low-dimensional chaos occurs when the second largest Lyapunov exponent Λ_2 becomes negative. Fig. 1(b) shows the five largest Lyapunov exponents versus ϵ for the full system Eq. (18), where we see that the system has only one positive exponent for $\epsilon > \epsilon_c \approx 0.065$. Apparently, we have $\epsilon_c \approx \epsilon_c^T$, indicating that the onset of low-dimensional chaos coincides with the onset of stable synchronization among the three chaotic oscillators. We also note that, at ϵ_c, Λ_2 and Λ_3 both become zero and for $\epsilon > \epsilon_c$, they degenerate to the negative Lyapunov exponent of the uncoupled attractor. This behavior is caused by the degeneracy of the nontrivial eigenvalues of the coupling matrix **G** and is therefore nongeneric. As we will see later, introducing a small amount of symmetry-breaking, such as making the oscillators slightly nonidentical, can immediately remove the degeneracy in the Lyapunov exponents at and after the bifurcation to low-dimensional chaos.

3.2. Nonidentical Rössler oscillators

When the oscillators are not identical, the direct synchronization state $(x_1, y_1, z_1) = (x_2, y_2, z_2) = (x_3, y_3, z_3)$ is no longer a solution of the system and, hence, it is not an invariant subspace of the system. In this case, we expect generalized synchronization. Investigation of a system of *two* coupled Rössler oscillators indicates that the generalized synchronization can manifest itself in the form of time-lagged synchronization [16]. To our knowledge, time-lagged synchronization in systems consisting of more than two coupled chaotic oscillators has not been addressed previously. Here we demonstrate, for a system of N ($N > 2$) coupled nonidentical Rössler oscillators, that the occurrence of low-dimensional chaos is accompanied by the onset of such a lag synchronization among these oscillators.

Some features of the lag synchronization, when the number of coupled oscillators is more than two, are as follows. In general, we say there is a lag synchronization between oscillator i and j if there exists a lag time $\tau_{ij}^{\min} \neq 0$ such that

$$\left|\mathbf{x}_j(t + \tau_{ij}^{\min}) - \mathbf{x}_i(t)\right| \to 0, \quad \text{as } t \to \infty, \tag{21}$$

where the lag time $\tau_{ij}^{\min}$ is approximately proportional to the mismatch between the two oscillators [16]. If the N oscillators are coupled along a circle (periodic boundary condition), then the lag times between the adjacent oscillators satisfy:

$$\tau_{1N}^{\min} = \tau_{12}^{\min} + \tau_{23}^{\min} + \cdots + \tau_{(N-1)N}^{\min}. \tag{22}$$

The following similarity functions [16] provides a convenient way to detect lag synchronization:

$$S_{ij}(\tau) = \sqrt{\frac{\left\langle \left[x_j(t+\tau) - x_i(t)\right]^2 \right\rangle}{\left[\langle x_i^2(t)\rangle \langle x_j^2(t)\rangle\right]^{1/2}}}, \quad i, j = 1, \ldots, N \ \ (i \neq j), \tag{23}$$

where x is a dynamical variable of the the Rössler oscillator, τ is a time delay, and $\langle\cdot\rangle$ denotes time average. Let $S_{ij}^{\min}$ be the minimum value of $S_{ij}(\tau)$. The lag time $\tau_{ij}^{\min}$ is thus the time delay at which $S_{ij}^{\min}$ is minimum. Lag synchronization between oscillators i and j is thus defined by the condition: $S_{ij}^{\min} = 0$ and $\tau_{ij}^{\min} \neq 0$. In contrast, a complete synchronization is characterized by: $S_{ij}^{\min} = 0$ and $\tau_{ij}^{\min} = 0$.

In the following, we emphasize our point, by numerical experiments, that when the coupling parameter is increased through a critical value so that the transition to low-dimensional chaos occurs, lag synchronization among the coupled oscillators occurs. For clarity of presentation, we report numerical experiments using $N = 3$. To introduce mismatch among the oscillators, we choose ω_i ($i = 1, 2, 3$) randomly in the interval [0.95,1.05]. For the results in this Section, the values of ω_i are: $\omega_1 \approx 1.003$, $\omega_2 \approx 0.978$ and $\omega_3 \approx 1.037$. Fig. 2(a) shows part of the Lyapunov spectrum (the first five exponents) versus the coupling parameter ϵ. Ignoring periodic windows, we see that low-dimensional chaos occurs at $\epsilon_c \approx 0.08$ as there is only one positive Lyapunov exponent for $\epsilon > \epsilon_c$. Fig. 2(b)–(d) show $S_{12}^{\min}$, $S_{13}^{\min}$, and $S_{23}^{\min}$ versus ϵ, respectively. We see that when the coupling is small, the values of $S_{12}^{\min}$, $S_{13}^{\min}$, and $S_{23}^{\min}$ are large, indicating a lack of any synchronization. As ϵ is increased through ϵ_c, the values of $S^{\min}$ become approximately zero, indicating the occurrence of synchronization. This synchronization is, however, time lagged, as can be seen from Fig. 3(b)–(d), the plots of $\tau_{12}^{\min}$,

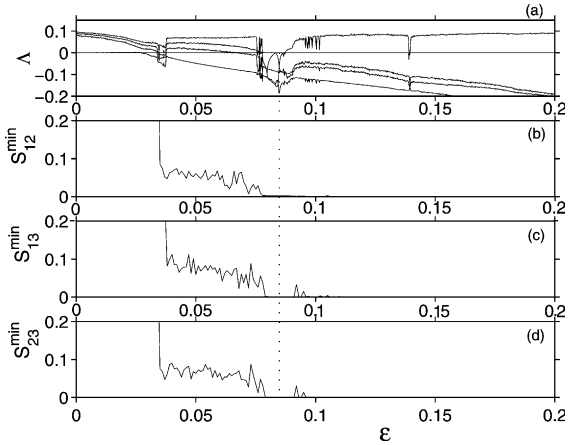

Fig. 2. For Eq. (18) with $N = 3$ (system of three coupled nonidentical Rössler oscillators): (a) the first five Lyapunov exponents versus ϵ; (b–d) the minimum values of the similarity functions $S_{12}^{\min}$, $S_{13}^{\min}$, and $S_{23}^{\min}$ versus ϵ, respectively. The nearly zero values of these quantities indicate the presence of synchronization for $\epsilon > \epsilon_c$.

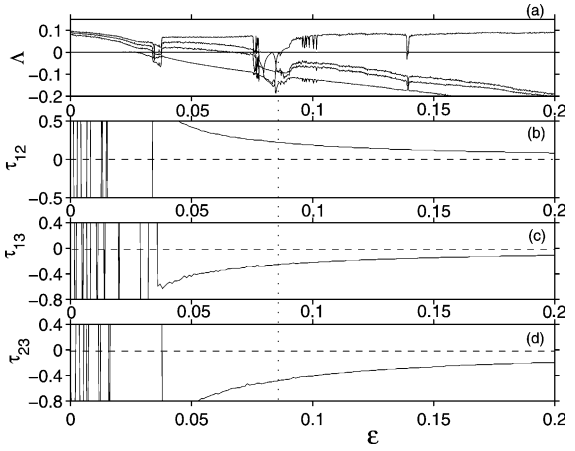

Fig. 3. For Eq. (18) with $N = 3$ (system of three coupled nonidentical Rössler oscillators): (a) the first five Lyapunov exponents versus ϵ; (b–d) the lag times $\tau_{12}^{\min}$, $\tau_{13}^{\min}$, and $\tau_{23}^{\min}$ versus ϵ, respectively. Nonzero values of the lag times for $\epsilon > \epsilon_c$ indicate chaotic lag synchronization.

$\tau_{13}^{\min}$, and $\tau_{23}^{\min}$ versus ϵ. We see that these lag times are not zero for $\epsilon > \epsilon_c$ where the minimum values of the similarity functions are already zero. In fact, for $\epsilon \gtrsim \epsilon_c$, the lag times are about 0.25, corresponding to about 10% of the average period of the oscillations of the dynamical variables in the Rössler oscillators. The occurrence of lag synchronization for $\epsilon > \epsilon_c$ can also be explicitly seen by examining the phase-space trajectories. Fig. 4(a), (c) and (e) show for $\epsilon = 0.011$, $x_1(t)$ versus $x_2(t)$, $x_1(t)$ versus $x_3(t)$, and $x_2(t)$ versus $x_3(t)$, respectively. Clearly, there is no direct synchronization among $x_1(t)$, $x_2(t)$, and $x_3(t)$ as the plots spread away from the diagonal lines. However, when the proper lag times are taken into account, the plots are confined in the neighborhood of the diagonal lines, as shown in Fig. 4(b), (d) and (f), the plots of $x_1(t)$ versus $x_2(t + \tau_{12}^{\min})$, $x_1(t)$ versus $x_3(t + \tau_{13}^{\min})$, and $x_2(t)$ versus $x_3(t + \tau_{23}^{\min})$, respectively. Note that the lag times are: $\tau_{12}^{\min} \approx 0.17$ (Fig. 4(b)), $\tau_{13}^{\min} \approx -0.2$ (Fig. 4(d)), and $\tau_{23}^{\min} \approx -0.37$ (Fig. 4(f)), which satisfy $\tau_{12}^{\min} + \tau_{23}^{\min} \approx \tau_{13}^{\min}$, as stipulated by Eq. (22).

The relationship between the onsets of low-dimensional chaos and synchronism can be seen more explicitly by computing the following *synchronization bifurcation diagram*, taking into account the proper time lags. We vary the coupling parameter systematically in the interval that contains the transition from high-dimensional to low-dimensional chaos. For each parameter value, we compute the similarity functions $S_{ij}(\tau)$ $(i, j = 1, \ldots, N, i \neq j)$ to obtain the proper

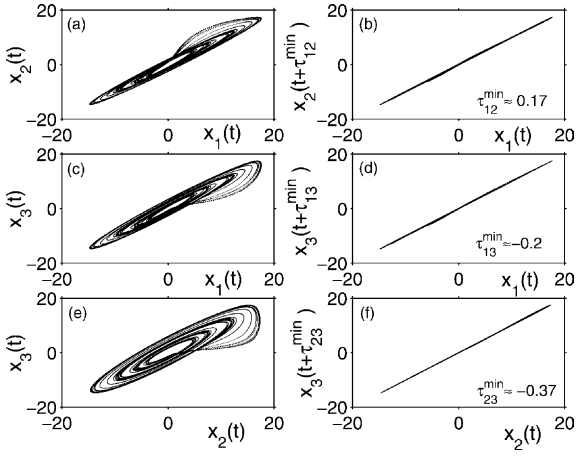

Fig. 4. For Eq. (18) with $N = 3$ (system of three coupled nonidentical Rössler oscillators), lag synchronization at $\epsilon = 0.011$. (a,c,e) $x_1(t)$ versus $x_2(t)$, $x_1(t)$ versus $x_3(t)$, and $x_2(t)$ versus $x_3(t)$, respectively; (b,d,f) $x_1(t)$ versus $x_2(t + \tau_{12}^{\min})$, $x_1(t)$ versus $x_3(t + \tau_{13}^{\min})$, and $x_2(t)$ versus $x_3(t + \tau_{23}^{\min})$, respectively.

lag times $\tau_{ij}^{\min}$. The asymptotic values of the lag-time-adjusted difference in the dynamical variables from individual oscillators

$$\Delta x_{ij}^{\tau} = x_j\left(t + \tau_{ij}^{\min}\right) - x_i(t), \quad i, j = 1, \ldots, N, \;\; i \neq j$$

are then computed. Fig. 5(b)–(d) show, for $N = 3$, Δx_{12}^{τ}, Δx_{13}^{τ}, and Δx_{23}^{τ} versus ϵ, respectively. Apparently, the numerically computed, lag-time adjusted values of Δx^{τ}'s become approximately zero after the system becomes low-dimensionally chaotic. In contrast, if the lag times are not taken into account, the bifurcation diagrams show no sign of synchronization, as shown in Fig. 6(a)–(c), where $\Delta x_{12}^{\tau=0}$, $\Delta x_{13}^{\tau=0}$, and $\Delta x_{23}^{\tau=0}$ versus ϵ are plotted.

The above results suggest that the synchronization pattern in coupled nonidentical chaotic oscillators is generally quite complicated. The results, however, provide a strong credance to our proposition that the occurrence of low-dimensional chaos in high-dimensional phase space is fundamentally related to chaos synchronism.

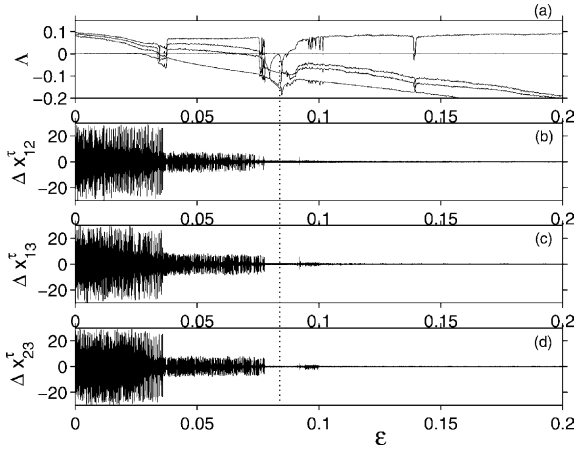

Fig. 5. For Eq. (18) with $N = 3$ (system of three coupled nonidentical Rössler oscillators), bifurcation diagram of lag synchronization. (b–d) Δx_{12}^{τ}, Δx_{13}^{τ}, and Δx_{23}^{τ} versus ϵ, respectively.

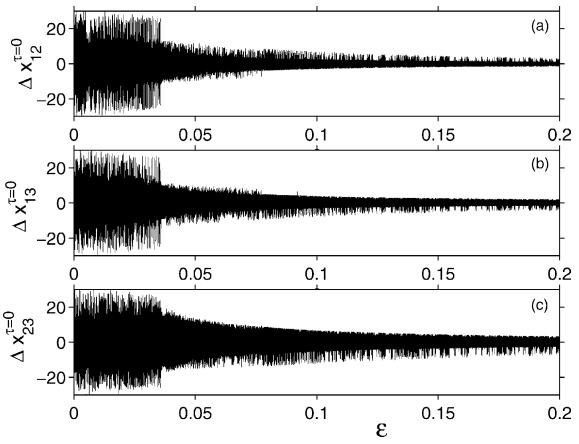

Fig. 6. For Eq. (18) with $N = 3$ (system of three coupled nonidentical Rössler oscillators), bifurcation diagram of the difference among dynamical variables. (a–c) $\Delta x_{12}^{\tau=0}$, $\Delta x_{13}^{\tau=0}$, and $\Delta x_{23}^{\tau=0}$ versus ϵ, respectively. There exists apparently no direct synchronization between the coupled oscillators.

4. Low-dimensional chaos in spatially extended systems

We demonstrate here that the fundamental interplay between low-dimensional chaos and synchronism can also be expected in a discretized model derived from a nonlinear PDE. In particular, we consider the following one-dimensional PDE that describes the propagation of nonlinear waves in forced, spatially extended medium with dispersion characterized by medium susceptibility σ_1 and σ_2, and damping γ [7]

$$\frac{\partial^2 \Phi}{\partial t^2} = -\gamma \frac{\partial \Phi}{\partial t} - \sigma_1 \Phi^3 + \sigma_2 \Phi + \epsilon \frac{\partial^2 \Phi}{\partial z^2} + f \sin \omega t, \tag{24}$$

where $\Phi(z,t)$ is the local displacement of the medium, ϵ is a quantity related to the group velocity of the wave, and f and ω are the forcing amplitude and frequency, respectively. In order to solve Eq. (24) numerically, one discretizes it spatially by the following substitutions

$$\begin{aligned} &z \to i, \\ &\Phi(z,t) \to x^i(t), \\ &\frac{\partial^2 \Phi}{\partial z^2} \to \mathrm{D}_2 = x^{i+1} - 2x^i + x^{i-1}, \end{aligned} \tag{25}$$

where i is an integer denoting the spatial site, x^i is the medium displacement at site i, and D_2 is the discrete second-order differential operator. Eq. (24) thus becomes the following set of coupled ordinary differential equations:

$$\frac{\mathrm{d}^2 x^i(t)}{\mathrm{d}t^2} = -\gamma \frac{\mathrm{d}x^i(t)}{\mathrm{d}t} - \sigma_1 (x^i(t))^3 + \sigma_2 x^i(t) + f \sin \omega t + \epsilon \mathrm{D}_2[x^i(t)], \quad i = 1, \ldots, N. \tag{26}$$

Letting $y^i(t) \equiv \mathrm{d}x^i(t)/\mathrm{d}t$ and $z^i(t) = \omega t$, we can convert Eq. (26) into a set of coupled, first-order equations. Taking into account the effect of spatial inhomogeneity of the medium and nonuniformity of the external force in space, we obtain the following:

$$\begin{aligned} &\frac{\mathrm{d}x^i(t)}{\mathrm{d}t} = y^i(t), \\ &\frac{\mathrm{d}y^i(t)}{\mathrm{d}t} = -\gamma^i \frac{\mathrm{d}x^i(t)}{\mathrm{d}t} - \sigma_1^i (x^i(t))^3 + \sigma_2^i x^i(t) + f^i \sin z^i + \epsilon \mathrm{D}_2[x^i(t)], \\ &\frac{\mathrm{d}z^i(t)}{\mathrm{d}t} = \omega^i, \quad i = 1, \ldots, N, \end{aligned} \tag{27}$$

which is the set of coupled Duffing oscillators [17].

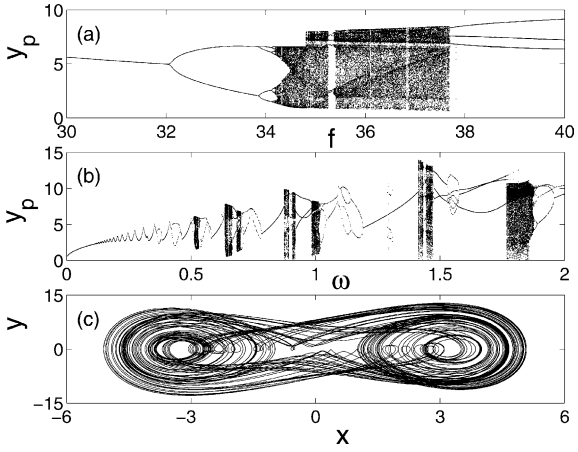

Fig. 7. Bifurcation diagrams of the single Duffing oscillator in Eq. (27) for $\gamma = 0.3$, $\sigma_1 = \sigma_2 = 1.0$: (a) y_p versus f for $\omega = 1.0$ and (b) y_p versus ω for $f = 36.0$, where y_p is the y-value obtained on the Poincaré surface of section defined by $x = 0$. (c) For $f = 36.0$ and $\omega = 1.0$, projection of the Duffing chaotic attractor in the (x, y)-plane.

Fig. 7(a) and (b) show the bifurcation diagrams of a single Duffing oscillator, where $y(t)$ versus f and ω on the Poincaré surface of section defined by $x = 0$ are plotted, respectively. There are apparently extensive parameter regions for chaotic attractors. Fig. 7(c) shows the projection of the chaotic attractor in the (x, y)-plane for $f = 36.0$ and $\omega = 1.0$. To explore the interplay between synchronization and low-dimensional chaos, we couple $N = 15$ such Duffing chaotic oscillators, as in Eq. (27). Fig. 8(a) and (b) show part of the transverse and full Lyapunov spectra, respectively. In particular, in Fig. 8(a), the two largest, distinct transverse exponents, together with the constant positive exponent of the single Duffing oscillator in the synchronization manifold, are shown. We see that stable synchronous chaos arises for $\epsilon > \epsilon_c \approx 12.0$. In Fig. 8(b), the first five largest exponents from the full system are plotted, where we see that, despite periodic windows and fluctuations of the exponents near the edges of these windows [18], for $\epsilon > \epsilon_c$ there is apparently only one positive exponent, signifying low-dimensional chaos. Fig. 8(a) and (b) thus provide qualitative evidence for the interplay between the onsets of low-dimensional chaos and synchronization in dynamical systems described by nonlinear PDEs.

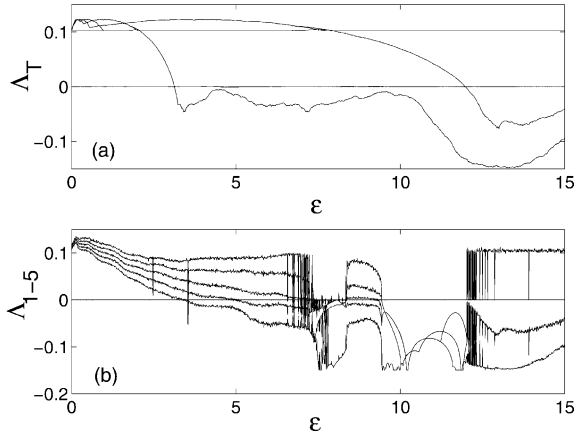

Fig. 8. For the system of $N = 15$ coupled Duffing chaotic oscillators for the same set of parameter values as in Fig. 7(c). (a) the first two distinct largest transverse Lyapunov exponents versus the coupling parameter ϵ. The constant positive exponent is the largest Lyapunov exponent of a single Duffing chaotic oscillator in the synchronization manifold. Synchronization occurs at $\epsilon \approx 12.0$. (b) The first five exponents from the full Lyapunov spectrum versus ϵ. Despite periodic windows and fluctuations of the exponents near the windows, there exists only one positive Lyapunov exponent, indicating the occurrance of low-dimensional chaos after onset of synchronization.

5. Generalized synchronization and the onset of low-dimensional chaos

When the coupled chaotic dynamics are characteristically different, e.g., when $\mathbf{f}$ and $\mathbf{g}$ are distinct in Eq. (3), we expect generalized synchronization, i.e., $\mathbf{y} = \mathbf{h}(\mathbf{x})$, to occur at sufficiently strong coupling. Typically, we expect the occurrence of generalized synchronization to coincide with the onset of low-dimensional chaos as the coupling parameter is increased from zero.

A technical issue is how to detect the occurrence of generalized synchronization. The function $\mathbf{y} = \mathbf{h}(\mathbf{x})$ can be difficult to detect because it may be nondifferentiable and complicated [19,20]: it can even be a fractal [21]. Here we make use of the criterion based on examining the relationship between the distance of nearest neighbors in the $\mathbf{x}$ and $\mathbf{y}$ space, which was proposed by Rulkov et al. [19]. The general idea is that if there exists a generalized synchronization and $\mathbf{y} = \mathbf{h}(\mathbf{x})$ is a continuous function, then, when two points $\mathbf{x}_1(t)$ and $\mathbf{x}_2(t)$ in $\mathbf{x}$ get close at time t, the corresponding points $\mathbf{y}_1(t)$ and $\mathbf{y}_2(t)$ in $\mathbf{y}$ will be close, too, and vice versa. One can then examine the statistical average of the following ratio:

$$R_{xy} \equiv \lim_{|\Delta\mathbf{x}|\to\mathbf{0}} \left\langle \frac{|\Delta\mathbf{y}|}{|\Delta\mathbf{x}|} \right\rangle, \tag{28}$$

where $\langle\cdot\rangle$ denotes the ensemble average, i.e., average over many chaotic trajectories. If there is no synchronization between $\mathbf{x}$ and $\mathbf{y}$, the ratio R_{xy} will be infinite (mathematically). On the other hand, if there exists a generalized synchronization, R_{xy} will be finite. In computer simulations, however, R_{xy} will in general be larger than $1/\delta_0$, where δ_0 is the computer roundoff, in the absence of synchronization. A reduction from $1/\delta_0$ in R_{xy} indicates the onset of generalized synchronization. In practice, one usually computes both ratios R_{xy} and R_{yx} and examine their product

$$R = R_{xy}R_{yx}. \tag{29}$$

To illustrate the interplay between generalized synchronization and the onset of low-dimensional chaos, we investigate a system of two coupled, but distinct, maps, which is derived from a physical model. In particular, we consider the dynamics of floaters convected on the surface of an incompressible flow [22]. Let $\mathbf{v}$ be the velocity field, where $\nabla \cdot \mathbf{v} = 0$, and let $v_z = az$ so that $\partial_x v_x + \partial_y v_y = -a$. The trajectories of the particles on the surface of this fluid ($z = 0$) are

$$\frac{\mathrm{d}x}{\mathrm{d}t} = v_x, \quad \frac{\mathrm{d}y}{\mathrm{d}t} = v_y. \tag{30}$$

Any initial area on the surface of the fluid (the (x, y) plane) contracts exponentially with time. We choose the following velocity field: $\mathbf{v} = \mathbf{v}_1 + \mathbf{v}_2 + \mathbf{v}_3$, where the three components of $\mathbf{v}$ are chosen to be

$$\begin{aligned} \mathbf{v}_1 &= -ay(t)\mathbf{y}_0, \\ \mathbf{v}_2 &= y(t)\mathbf{x}_0, \\ \mathbf{v}_3 &= \mathbf{y}_0 \sin\left[x(t) + 2\pi z(t)\right] \cdot \left[k \sum_{n=-\infty}^{\infty} \delta(t-n)\right]. \end{aligned} \tag{31}$$

In Eq. (31), v_1 is a contractive component, v_2 is a shear flow, and v_3 is a periodic vortical flow component with period 1. The quantity, $\delta(t-n)$ is a delta function and $z(t)$ is a random variable. Solving Eq. (30), we obtain the position of a particle after time $t = n+1$ in terms of the position at time $t = n$,

$$\begin{aligned} x_{n+1} &= \left[x_n + \frac{1-e^{-a}}{a} y_n\right] \mathrm{mod}(2\pi), \\ y_{n+1} &= e^{-a} y_n + k \sin\left(x_{n+1} + 2\pi z_n\right). \end{aligned} \tag{32}$$

If $z_n = 0$, Eq. (32) is known as the Zaslavsky map, which can exhibit chaotic attractors [23]. The case where z_n is a random variable was treated previously in Ref. [22]. In order to study generalized synchronization, we choose z_n to be a chaotic variable defined by

$$z_{n+1} = rz_n(1 - z_n) + \epsilon y_n. \tag{33}$$

The term $2\pi z_n$ represents the coupling from the z-dynamics, which is the logistic map with a term ϵy_n describing the coupling from the (x, y) dynamics. We regard the (x, y) map and the z map as two coupled systems that are apparently quite different. The full system, which is a three-dimensional map, can possess chaotic attractors with both one and two positive Lyapunov exponents. The transition from high- to low-dimensional chaos is treated in Refs. [24–26]. Here we wish to address the interplay between the transition and generalized synchronization.

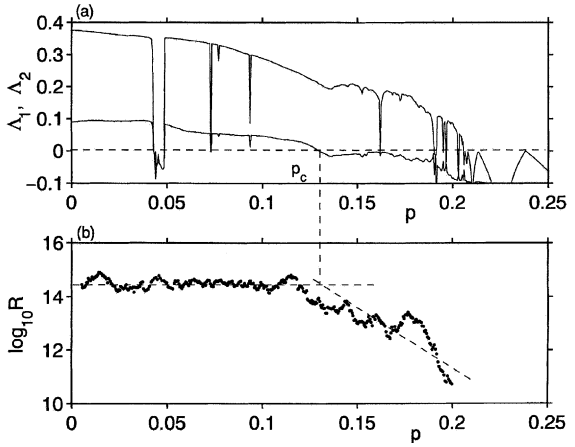

Fig. 9. For the coupled map system Eqs. (32) and (33): (a) the first two Lyapunov exponents versus the parameter p, and (b) the ratio R of the nearest-neighbor distance versus p. Values of R near the inverse of the computer roundoff suggests lack of synchronization, and a decrease of R from the inverse indicates the onset of generalized synchronization. We see that the onset of generalized synchronization roughly coincides with the transition to low-dimensional chaos.

In numerical experiments, we fix $k = 0.5$ and $\epsilon = 0.01$ and study the transition in the two-dimensional parameter space (r, a). Let $\mathscr{L}$ be the line segment from $(r_1, a_1) = (3.75, 0.05)$ to $(r_2, a_2) = (3.55, 0.2)$, and let p be the distance from (r_1, a_1) along the line segment. Fig. 9(a) shows the two largest Lyapunov exponents of the asymptotic set versus p, where we see that the transition from high- to low-dimensional chaos occurs at $p_c \approx 0.13$. Fig. 9(b) shows the ratio $R = R_{xy,z}R_{z,xy}$ versus p, where $R_{xy,z}$ and $R_{z,xy}$ are averaged over 100 trajectories, each of 10^5 points. For $p < p_c$ where the system is high-dimensionally chaotic, the value of R remains high and constant ($>10^{14}$), which is approximately the inverse of the computer roundoff. The value of R begins to decrease roughly as p increases through p_c when the system becomes low-dimensionally chaotic, signifying the onset and the gradual enhancement of generalized synchronization between the (x, y)-dynamics and the z-dynamics. The result suggests that for chaotic dynamics coming from characteristically different maps, the onsets of low-dimensional chaos and generalized synchronization coincide.

6. Discussion

The development and success of low-dimensional chaotic dynamics are meaningful when the dynamical invariant sets of the underlying physical system are low-dimensional. Indeed, many dynamical systems, despite their high dimensionality, exhibit low-dimensionally chaotic attractors [1,2] for which a good understanding can be achieved and strategies for control and even prediction can be formulated. High-dimensionally chaotic systems with multiple positive Lyapunov exponents, on the other hand, are still poorly understood and there exists no satisfactory general solution for control, synchronization, and prediction. Understanding the mechanism of how low-dimensionally chaotic dynamics arises in high-dimensional phase space is thus important, because it will help provide insights to understanding high-dimensional chaos in general.

This paper provides understanding for a possible scenario for dynamical systems to exhibit low-dimensional asymptotic chaotic invariant set. The key is synchronization. We provide arguments and strong numerical evidence for our conclusion, which can be casted in the following conjecture: generalized chaotic synchronism is a sufficient condition for the occurrence of low-dimensionally chaotic invariant sets in high-dimensional phase space. Our results may provide an explanation for the observation of low-dimensionally chaotic sets in infinitely dimensional phase space such as those arising from nonlinear PDEs.

Acknowledgements

We thank L. Sauter for discussions during the initial phase of the project. YCL and ZL are supported by AFOSR under grant no. F49620-98-1-0400 and by NSF under grant no. PHY-9996454. EMB is supported by NSF under grant no. DMS-0071314.

References

[1] Ruelle D, Takens F. Commun Math Phys 1971;20:167.
[2] There are so many examples of low-dimensionally chaotic dynamics occurring in high-dimensional phase space that we do not attempt to give even a partial list of the literature. An example is the magnetic ribbon system that has been used to verify a variety of low-dimensionally chaotic phenomena. See, for instance Ditto WL et al. Phys Rev Lett 1989;63:923;
and Ditto WL, Rauseo SN, Spano ML. Phys Rev Lett 1990;65:3211.
[3] Eckmann J-P, Ruelle D. Rev Mod Phys 1985;57:617.
[4] Kantz H, Schreiber T. Nonlinear time series analysis. Cambridge: Cambridge University Press; 1997.
[5] Fujisaka H, Yamada T. Prog Theor Phys 1983;69:32;
Afraimovich VS, Verichev NN, Rabinovich MI. Radio Phys Quantum electron 1986;29:747.
[6] While the phenomenon of synchronous chaos was first reported in Ref. [5], it was independently discovered and it was pointed out for the first time in the following paper that the phenomenon can have potential application in nonlinear digital communication Pecora LM, Carroll TL. Phys Rev Lett 1990;64:821;
Since then, synchronization in chaotic systems has become one of the most active research areas in nonlinear dynamics. See, for example Ditto WL, Showalter K. Chaos (Focus Issue on Control and Synchronization of Chaos) 1997;7:509.
[7] Umberger DK, Grebogi C, Ott E, Afeyan B. Phys Rev A 1989;39:4835.
[8] See, for example Parlitz U, Chua LO, Kocarev L, Halle KS, Shang A. Int J Bifurcat Chaos 1992;2:973;
Cuomo KM, Oppenheim AV. Phys Rev Lett 1993;71:65;
Cuomo KM, Oppenheim AV, Strogatz SH. Int J Bifurcat Chaos 1993;3:1629;
Short KM. Int J Bifurcat Chaos 1994;4:957;
Short KM. Int J Bifurcat Chaos 1996;6:367.
[9] Recent works on communicating with chaos include Baptista MS, Macau EE, Grebogi C, Lai Y-C, Rosa E. Phys Rev E 2000;62:4835;
Chen C-C, Yao K. IEEE Commun Lett 2000;4:37;
Sushchik M, Rulkov N, Lason L, Tsimring L, Abarbanel H, Yao K, Volkovskii A. IEEE Commun Lett 2000;4:128;
Chen C-C, Yao K. IEEE Trans Circuits Systems I 2000;47:1663.
[10] There are many books on synergetics. See, for example Haken H. Synergetics—an introduction: nonequilibrium phase transitions and self-organization in physics, chemistry and biology. Berlin: Springer-Verlag; 1978;
Haken H. Advanced synergetics: instability hierarchies of self-organizing systems and devices. Berlin: Springer-Verlag; 1983.
[11] Bushev M. Synergetics: chaos, order, and self-organization. Singapore: World Scientific; 1994.
In Chapter 11 of this book, which is entitled ''Chaos-Invalidity of the Slaving Principle,'' the author states: ''It is intuitively clear that order is related to specific bans, to restrictions, while chaos is a violation of restrictions. The restrictions, enforced by the slaving principle, are violated by chaos owing to the fact that the difference disappears between stable and unstable modes. When there is chaos, practically all modes are unstable (slow). Chaos is persistent instability.''.
[12] Rössler OE. Phys Lett A 1976;57:397;
Rössler OE. Phys Lett A 1979;71:155.
[13] Rulkov NF, Sushchik MM, Tsimring LS, Abarbanel HDI. Phys Rev E 1995;51:980;
Kocarev L, Parlitz U. Phys Rev Lett 1996;76:1816;
Abarbanel HDI, Rulkov NF, Sushchik M. Phys Rev E 1996;53:4528.
[14] Josić K. Phys Rev Lett 1998;80:3053.
[15] Heagy JF, Carroll TL, Pecora LM. Phys Rev Lett 1994;73:3528;
Heagy JF, Pecora LM, Carroll TL. Phys Rev Lett 1995;74:4185;
Pecora LM, Carroll TL. Phys Rev Lett 1998;80:2109.
[16] Rosenblum MG, Pikovsky AS, Kurths J. Phys Rev Lett 1997;78:4193;
Taherion S, Lai Y-C. Phys Rev E 1999;59:R6247.
[17] Moon FC. Phys Rev Lett 1984;53:962;
Moon FC, Li G-X. Phys Rev Lett 1985;55:1439.
[18] These fluctuations come from multiple coexisting attractors and their complicated basin structures. See, for example Lai Y-C, Winslow RL. Phys Rev Lett 1994;72:1640;
Lai Y-C, Winslow RL. Physica D 1994;74:353.
[19] Rulkov NF, Sushchik MM, Tsimring LS, Abarbanel HDI. Phys Rev E 1995;51:980.
[20] Abarbanel HDI, Rulkov NF, Sushchik M. Phys Rev E 1996;53:4528;
Kocarev L, Parlitz U. Phys Rev Lett 1996;76:1816.
[21] Barreto E, So P, Gluckman BJ, Schiff SJ. Phys Rev Lett 2000;84:1689;
Barreto E, So P. Phys Rev Lett 2000;85:2490.
[22] Yu L, Ott E, Chen Q. Phys Rev Lett 1990;65:2935 Physica D 1991;53:102.
[23] Zaslavsky GM. Phys Lett A 1978;69:145.
[24] Kapitaniak T. Phys Rev E 1993;47:R2975.

[25] Harrison MA, Lai Y-C. Phys Rev E 1999;59:R3799;
Harrison MA, Lai Y-C. Int J Bifurcat Chaos 2000;10:1471;
Davidchack RL, Lai Y-C. Phys Lett A 2000;270:308.
[26] Kapitaniak T, Maistrenko Y, Popovych S. Phys Rev E 2000;62:1972;
Yanchuk S, Kapitaniak T. Phys Lett A 2001;290:139;
Yanchuk S, Kapitaniak T. Phys Rev E 2001;64:056235.